Improving High-Speed Machining Material Removal Rates by Rapid Dynamic Analysis

T. L. Schmitz[1], M. A. Davies[1] (2), K. Medicus[1], J. Snyder[2]
[1]Manufacturing Metrology Division, National Institute of Standards and Technology, Gaithersburg, MD
[2]Department of Mechanical Engineering and Engineering Science
University of North Carolina at Charlotte, Charlotte, NC

Abstract
Stability prediction and chatter avoidance in high-speed machining requires knowledge of the tool point dynamics. In this paper, three advances toward the rapid identification of the tool point frequency response and corresponding stable cutting parameters are described: 1) stable speeds determination using non-contact periodic impulsive excitation of the tool point (produced by spindle rotation and a stationary magnet) in conjunction with once-per-revolution sampling, 2) Receptance Coupling Substructure Analysis for the analytic prediction of the tool point response, and 3) once-per-revolution sampling of the audio signal during cutting to determine stability behavior.

Keywords: High speed machining, Material removal rate, Sub-structure analysis

1 INTRODUCTION

A primary objective of manufacturing operations is the efficient production of accurate parts. In the machine tool industry, significant research has focused on ways to increase material removal rates (MRR) without sacrificing workpiece accuracy. Two primary ways to raise MRR are to increase the: 1) cutting velocity, and 2) chip width. Research in the area of high-speed machining (HSM) addresses both issues [e.g., 1-4]. In HSM, spindle speeds are selected by considering the tool point dynamics. Several studies have shown that by taking advantage of the well-known lobing phenomenon and selecting a tooth passing frequency that is a substantial integer fraction of the natural frequency of the system's most flexible mode, MRR can be greatly increased [1, 5-8]. In the absence of significant tool wear, this simultaneously enables the selection of both high spindle speeds and large chip widths.

The limiting stability for a particular machining operation may be summarized using stability lobe diagrams, generated by various means, which indicate the chatter-free chip widths for a range of spindle speeds [5-7]. Inputs to the analytic or time-domain calculation of these diagrams include the cutting parameters, tool geometry, specific cutting energy coefficients, and the tool point frequency response function (FRF). Alternately, direct testing methods may be employed either off-line or in-process to directly determine stable cutting zones by experimental means [8].

As the use of HSM technology grows, particularly in companies that have moderate engineering support, the need to rapidly identify stability behavior using methods that do not require an extensive background in vibrations theory also increases. In these situations, partial information (e.g., optimum spindle speeds, but not allowable chip widths) is often all that is needed to greatly improve productivity. Measurements that provide this information may be performed prior to (pre-process) or during (in-process) machining. Clearly, the former has the advantage that a problem does not need to occur before it can be corrected.

In this paper, we describe three advances toward the rapid identification of HSM dynamics and/or stable cutting speeds. These include descriptions of two pre-process techniques, the *best speeds device* for determining optimum spindle speeds and Receptance Coupling Substructure Analysis for selection of the tool length giving maximized MRR, and a novel treatment of the in-process, synchronously sampled audio cutting signal. Comparisons with existing technologies are also provided.

2 STABILITY IDENTIFICATION METHODS

Three basic approaches are available for the selection of stable cutting parameters. First, pre-process experimental methods may be employed to: 1) measure the tool point FRF for a particular tool/holder/spindle combination and calculate the stability behavior using analytic or time-domain algorithms, or 2) directly determine the stable spindle speeds by cutting tests. Second, pre-process analytic techniques may be implemented to predict the tool point FRF and, again, use this predicted FRF as input to analytic or time-domain simulations. Third, in-process procedures can be adopted to monitor the cutting performance and suggest/implement changes to the cutting parameters (e.g., spindle speed).

2.1 Pre-process measurement

Three experimental techniques for pre-process stability behavior identification will be discussed here. First, dynamic testing can provide a quantitative measure of the tool point FRF and, subsequently, calculate the process stability using existing theories. However, this method can be time-consuming and inefficient. Recent research has also explored using a small explosive charge to automate the dynamic excitation and improve process repeatability [9].

Alternatively, we have utilized the rotation of the spindle itself to produce an impulsive excitation at a known and variable frequency by placing a magnet (or other suitable force actuator) in close proximity to the tool point. This

system relies on the well-known equation describing the most stable cutting speeds, Ω_j (in rpm),

$$\Omega_j = \frac{60 f_n}{j N_f}, \; j = 1, 2, 3 \ldots \quad (1)$$

where f_n is the natural frequency of the most flexible system mode (in Hz) and N_f is the number of flutes. As the rotating cutter teeth pass the magnet, a small impulsive force is periodically applied to the tool, generating a signal with energy content at the tooth passing frequency and its harmonics. When one of the harmonics of the tooth passing frequency aligns with the natural frequency of the system, a resonance results. These resonant conditions identically satisfy Equation 1, and, therefore, correspond to the most stable cutting speeds. In the simplest adaptation of this method, the resonances of the tool are detected qualitatively with a microphone as spindle speed is continuously ramped through the desired operating range. For the case of a single dominant mode, estimation of at least two stable speeds provides two equations and two unknowns (j and f_n). Using this information, the natural frequency *and, therefore, all stable speeds* of the system can be estimated directly from repeated application of Equation 1. Thus, it may be possible to determine the most stable spindle speeds in a matter of seconds using a magnet (or other suitable actuator), microphone, and electronics already residing in the machine controller. We believe that such a device could be integrated into machine tool controllers in a user-friendly configuration (similar to a tool length probe). This *best speeds device* concept is the subject of a U.S. patent application [10].

Initial testing of a more sophisticated adaptation of this idea has also shown encouraging results. In this work, once-per-revolution sampling was combined with an appropriately positioned optical displacement sensor and the non-contact magnetic excitation to determine the character of the real, or in-phase, portion of the tool point FRF (by sampling the tool displacement at peak force [11]) and identify stable spindle speeds. The setup for the tests is shown in Figure 1. A 12.7 mm diameter test bar, intended to simulate a two-flute endmill, was mounted in an HSK 63A collet-type holder with an overhang of 127 mm. To identify the tool point dynamics, the spindle speed was ramped linearly from rest to 15000 rpm in 2.5 s while the output from the optical displacement sensor and once-per-revolution signal were recorded. The tool displacement during spindle speed ramping (Figure 2) shows three regions of increased amplitude (at 1.6 s, 0.95 s, and 0.6 s) as harmonics of the tooth passing frequency sweep through the system natural frequency.

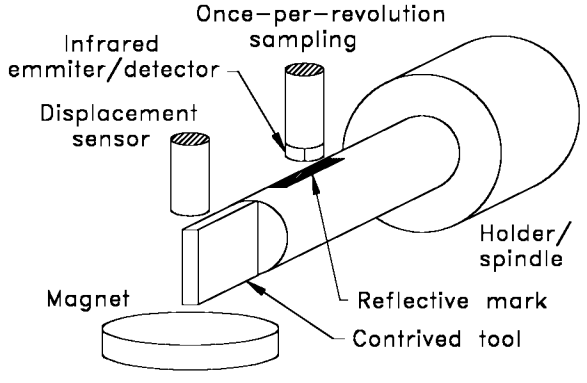

Figure 1: *Best speeds device* experimental setup.

Representative results for once-per-revolution sampling of the time series data are shown as a function of spindle speed in Figure 3. It is seen that the three resonances identified in the time series each have a qualitative character similar to the real portion of the FRF and are found at speeds of 11300 rpm, 7650 rpm, and 5800 rpm. The application of Equation 1 to these speeds shows that they correspond to the first three harmonics of the tooth passing frequency passing through the system natural frequency of approximately 764 Hz (verified by traditional dynamic testing using an instrumented hammer and accelerometer). Using the natural frequency information and the qualitative representation of the real part of the system FRF given by the once-per-revolution sampling (specifically, the section of data at spindle speeds greater than 11300 rpm), qualitative stability lobes were generated, as shown by the lower curve in Figure 3. A possible variation on this design includes mounting the optical probe through the magnet center to simplify setup.

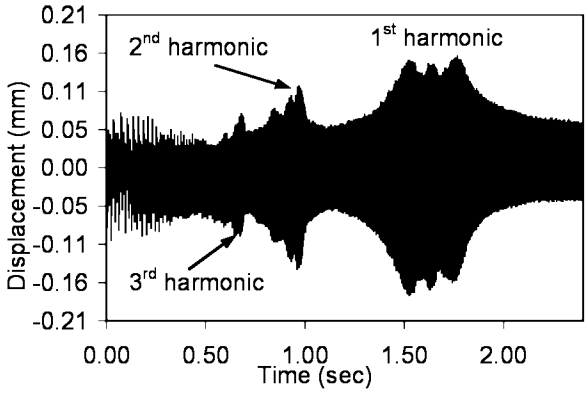

Figure 2: Optical sensor displacement.

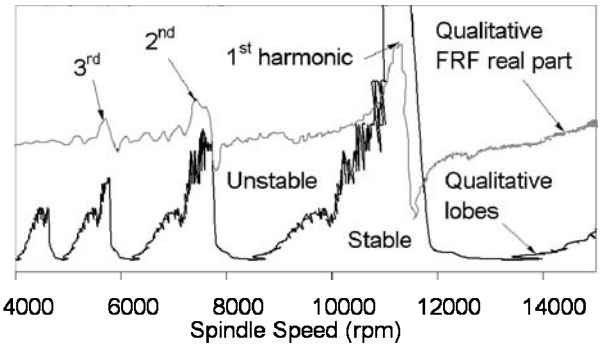

Figure 3: Qualitative stability behavior of contrived tool.

Finally, the optimum spindle speeds for a given tool/holder/spindle assembly may be determined by conducting a series of progressively deeper cuts (slotting is typical) to directly identify the dominant chatter frequency(s). One commercially available package uses a unidirectional microphone to sample the audio response during machining. Chatter is detected by filtering the tooth passing frequency and harmonics from the audio signal power spectrum and checking for remaining content. An appropriate spindle speed is then recommended if the cut is unstable [12]. In a similar manner to the *best speeds device* described in the previous paragraphs, this technique only provides optimum speeds, not quantitative stability lobes.

2.2 Pre-process prediction

We have also considered the application of Receptance Coupling Substructure Analysis (RCSA) to the prediction of the tool point FRF in HSM [13-16]. In this method, the FRF of the tool (derived from an analytic or finite-element based model) is coupled to an experimental FRF measurement of the holder/spindle through appropriate connections to determine the assembly FRF. Previous results have shown that the dynamic response after system changes may be predicted, thereby reducing the number of required measurements in some

applications. For example, RCSA is particularly relevant to *tool tuning* [17-19], a technique that modifies the system dynamics by adjusting the tool overhang length in an effort to improve MRR.

The RCSA model of the tool/holder/spindle assembly, shown in Figure 4, includes two components, the tool, *A*, and holder/spindle, *B*, connected by linear and rotational springs and dampers. Prediction of the tool point FRF, using this model, proceeds in three steps. First, the component frequency responses are obtained. The end mill is treated as a free-free beam with an appropriate cross-sectional profile and an analytic or finite-element model developed for the dynamic response (direct and cross FRFs are required at the two ends of the beam). Also, the selected holder is placed in the spindle and the free-end direct FRF measured (impact testing was used in this study). Second, the tool is placed in the holder/spindle and the connection parameters (k_x, c_x, k_θ, and c_θ) are identified using a single measurement and fit to the experimental data. Third, the complete system model is used to predict the tool point FRF for other tool lengths. As shown in Equation 2, the assembly tool point FRF, $G_{11}(\omega)$, is calculated from the component receptance and mobility terms and experimentally determined connection parameters. The receptance terms relate displacement to force, *H*, displacement to moment, *L*, rotation to force, *N*, and rotation to moment, *P*. The mobility terms (denoted *H'*, *L'*, *N'*, and *P'*) are defined similarly, but describe the time rate of the change of displacement and rotation to applied force and moment. Further details of the development of this equation are provided in reference [13].

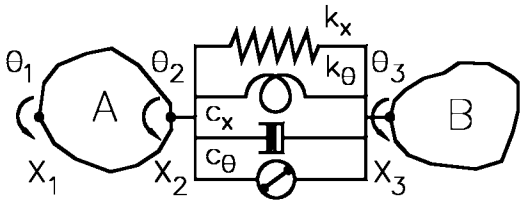

Figure 4: RCSA model for tool/holder/spindle assembly.

$$G_{11} = H_{11} - H_{12}E_1^{-1}E_2 - L_{12}E_3^{-1}\left(\left(k_\theta N_{21} + c_\theta N'_{21}\right) - E_4E_1^{-1}E_2\right)$$

where (2)

$$E_1 = \left(k_xH_{33} + k_xH_{22} + c_xH'_{33} + c_xH'_{22} + 1\right) - E_3^{-1}E_4$$
$$\left(k_xL_{33} + k_xL_{22} + c_xL'_{33} + c_xL'_{22}\right)$$
$$E_2 = \left(k_xH_{21} + c_xH'_{21}\right) - E_3^{-1}\left(k_\theta N_{21} + c_\theta N'_{21}\right)$$
$$\left(k_xL_{33} + k_xL_{22} + c_xL'_{33} + c_xL'_{22}\right)$$
$$E_3 = \left(k_\theta P_{33} + k_\theta P_{22} + c_\theta P'_{33} + c_\theta P'_{22} + 1\right)$$
$$E_4 = \left(k_\theta N_{33} + k_\theta N_{22} + c_\theta N'_{33} + c_\theta N'_{22}\right)$$

A particular application of the RCSA model is the identification of the tool length within the allowable overhang range that gives the highest MRR (possibly bounded by the available spindle torque and power [20]). An example of this capability will now be presented.

The tool for this example was a two-flute, 11.1 mm relieved neck diameter (12.7 mm shank diameter) carbide end mill with a 15.9 mm flute length and allowable overhang range of 112.5 mm to 124.0 mm. Following the RCSA algorithm, the tool and holder/spindle FRFs were identified first. The tool's direct and cross FRFs were calculated using the beam's equation of motion with appropriate boundary conditions [13] and analytic mode shapes from the literature [21]. The holder/spindle direct FRF was identified by impact testing. The tool was then placed in the HSK 63A collet-type holder at a mid-range overhang of 118.5 mm and the tool/holder/spindle assembly X-direction FRF measured. The connection parameters were estimated from a visual fit to this measurement and are shown in Table 1. The system model was then used to predict tool point FRFs over the full overhang range and the corresponding MRRs calculated using stability lobe theory [6].

k_x (N/m)	k_θ (N-m/rad)	c_x (N-s/m)	c_θ (N-m-s/rad)
$3.0\text{x}10^7$	$2.4\text{x}10^6$	239	67

Table 1: Stiffness/Damping Coefficients.

Comparisons between the predicted and measured tool point, Y-direction FRFs for the maximum and minimum overhang lengths are shown in Figures 5 and 6, respectively. Good qualitative agreement is seen. Figure 7 shows the variation in maximum MRR with tool length for an X-direction slotting cut when: 1) taking advantage of the lobing behavior, and 2) using the critical (or asymptotic) stability limit at a spindle speed of 20000 rpm. It is seen that the first curve suggests a best overhang of 122 mm (in this case, a lobe has been moved to the top spindle speed of 20000 rpm), while the second recommends 113.8 mm (this provides the dynamic absorber effect described previously [13], where the tool cantilever frequency is equal to a spindle natural frequency of 802 Hz and improved stability results). To verify the RCSA method predictive capability, stability lobes were generated from the predicted FRF for a 121 mm overhang and evaluated experimentally (full radial immersion milling in ISO AlMg1SiCu aluminum). Figure 8 shows the predicted lobes and machining results. The dramatic variation in allowable axial depth with spindle speed is verified. The required torque and power consumed for the 0.71 mm axial depth, 20000 rpm cut are 0.32 N-m and 0.67 kW, respectively, well within the capacity of the 20000 rpm/ 20kW spindle used in this study.

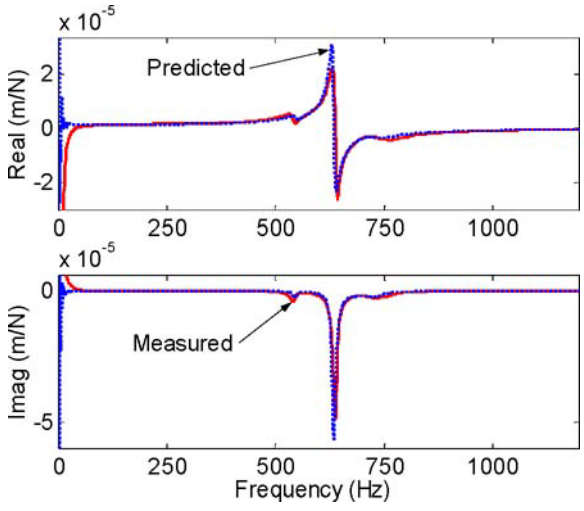

Figure 5: Predicted/measured FRF for 11.1 mm diameter, two flute, 124.0 mm overhang tooling.

2.3 In-process identification

The final fundamental method for chatter avoidance involves in-process evaluation of the cutting process. During cutting, the system response may be continuously tested for unstable behavior and the machining parameters adjusted if chatter is detected. The Chatter Recognition and Control (CRAC) system, for example, monitors the audio spectrum of the cutting process, applies a feed hold if chatter is sensed, and automatically adjusts the tooth passing frequency (or a low order harmonic of the tooth passing frequency,

depending on the maximum available spindle speed) to match the recorded chatter frequency [22].

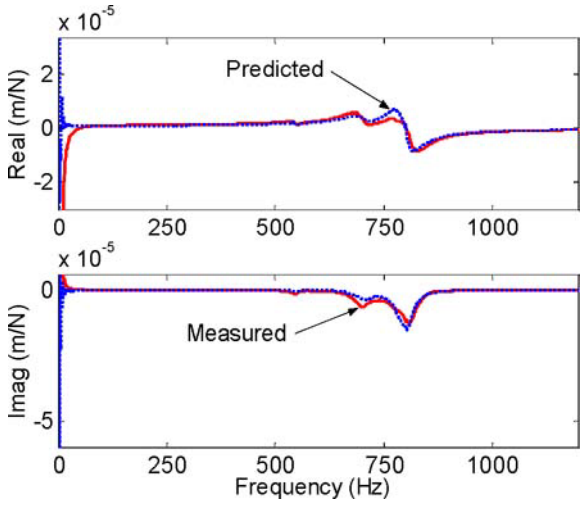

Figure 6: Predicted/measured FRF for 11.1 mm diameter, two flute, 112.5 mm overhang tooling.

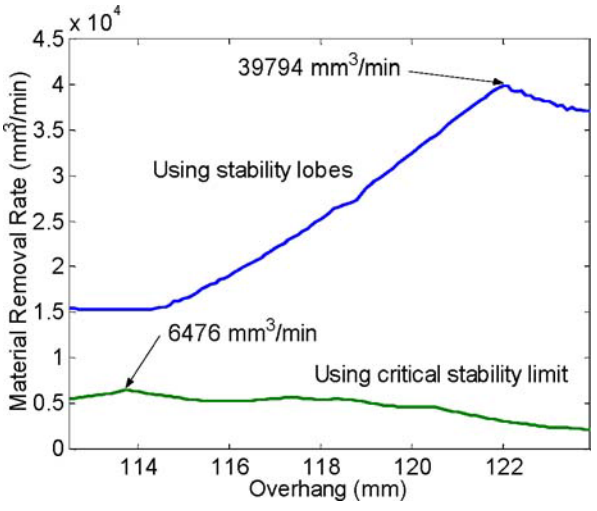

Figure 7: MRR variation with overhang length.

In a similar manner, we have recently implemented a technique that combines the audio signal during cutting with once-per-revolution sampling to identify unstable behavior. The fundamental concept is that stable cuts will generate content synchronous with spindle rotation and, therefore, a histogram of the periodically sampled audio signal will be characterized by a tightly spaced cluster of values (small variance). An unstable cut (due to regenerative chatter), on the other hand, will demonstrate asynchronous, or quasiperiodic, motion and give a more distributed set of audio samples (larger variance). This method is a derivative of the Poincaré sectioning technique described by Davies et al [18], where a Poincaré section of the x and y displacements of the tool point during cutting (obtained using an orthogonal pair of capacitance probes located near the tool tip) was analyzed for stable and unstable behavior. It was shown that stable cuts generated a series of closely grouped points (in the x-y plane) when the tool point motions were sampled at the spindle rotation frequency, while cuts experiencing regenerative chatter tended toward an elliptical point distribution, which is indicative of quasiperiodic motion.

To demonstrate this method of chatter detection, audio and synchronizing signals were recorded during slot machining of ISO AlZn5.5MgCu aluminum with an 11.8 mm diameter, two flute, carbide endmill. The overhang of the end mill from the HSK 63A holder face was 104 mm (approximately a 9:1 length to diameter ratio). Cutting data was obtained for both stable and unstable axial depths, 50 μm and 100 μm, respectively, at a spindle speed of 20000 rpm and chip load of 102 μm/tooth. These cuts bound the stability lobes, generated from impact testing and analytic simulation [6], at 20000 rpm as shown in Figure 9. This figure also includes histograms generated from the once-per-revolution sampling of the audio signals recorded during the cuts. The synchronizing signal was obtained using an infrared emitter-detector pair and a reflective mark on the tool (as shown in Figure 1). The stable 50 μm cut shows the expected close clustering of points and yields a variance of 0.00027 Volts^2. The unstable 100 μm cut exhibits a more widely distributed point spread and a 17.5 times increase in the calculated variance (0.0047 Volts^2).

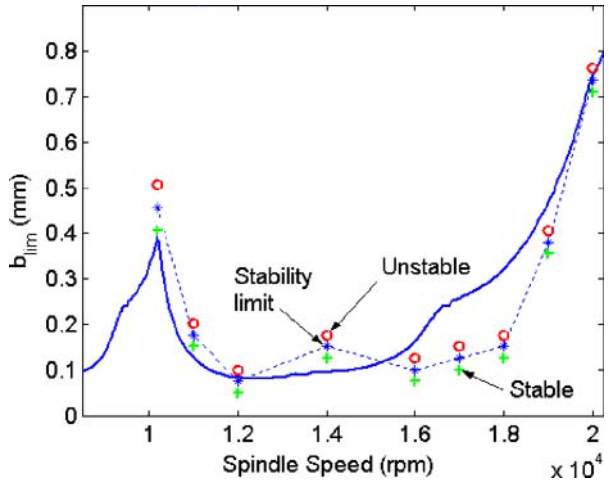

Figure 8: Stability lobe verification (11.1 mm diameter, 121.0 mm overhang, two flute endmill).

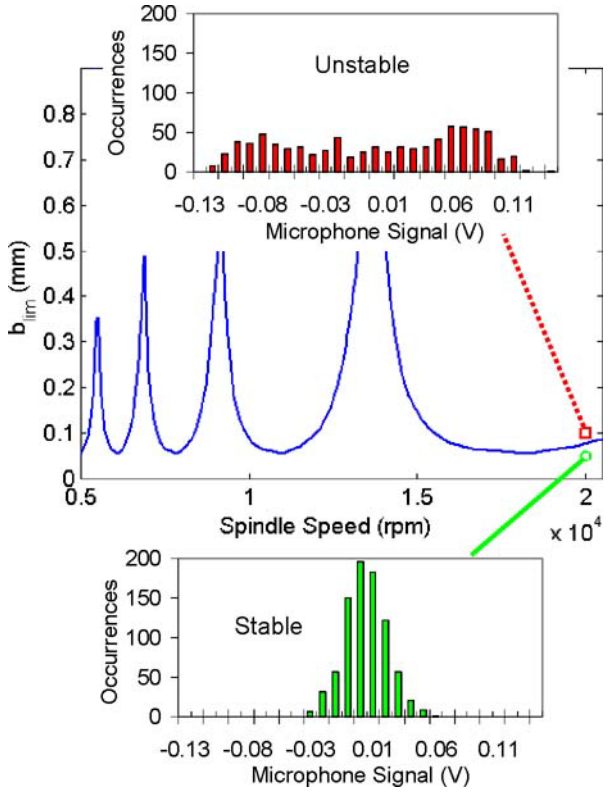

Figure 9: Stability lobe diagram for 11.8 mm diameter, 104 mm overhang, two flute endmill. Insets show histograms of synchronously sampled audio signals for stable (circle) and unstable (square) cuts.

In order to further demonstrate the utility of this technique, time domain milling simulation code, similar to that described by Tlusty [23], was written to produce the time series x and y direction tool point displacements, perform once-per-revolution sampling of the resultant displacement, construct the corresponding histograms, and calculate the variance. Additionally, the simulation used the tool point modal parameters (identified by impact testing) for the 9:1 tool and the same specific cutting force coefficients (600 MPa and 0.3) as applied in the generation of the stability diagram shown in Figure 9.

To determine the feasibility of the simulation, plots were generated showing the x vs. y tool point displacements and the once-per-revolution sampling of this data for axial depths of 50 μm (stable) and 100 μm (unstable). These plots are shown in Figures 10 and 11, respectively (note different scales). Reasonable agreement between these results and corresponding experimental data reported by Davies et al [18] was obtained.

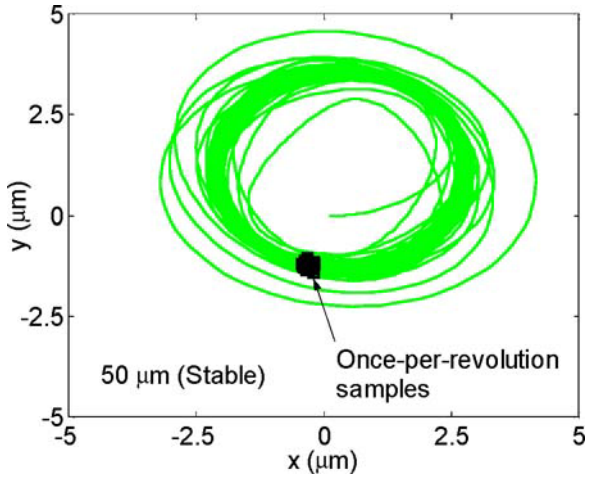

Figure 10: Simulated x vs. y displacements for 9:1 tooling (50 μm axial depth).

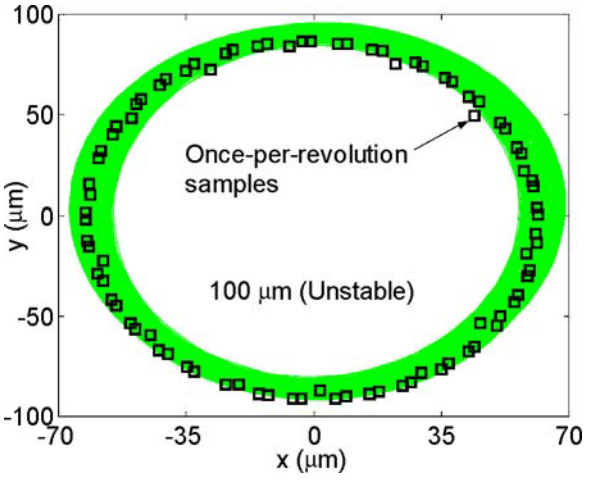

Figure 11: Simulated x vs. y displacements for 9:1 tooling (100 μm axial depth).

The empirically demonstrated increase in variance of unstable over stable cutting conditions shown in Figure 9 has also been explored in simulation. At a constant spindle speed of 20000 rpm, the axial depth was incremented from 50 μm to 100 μm in 5 μm steps and the resulting variance in the once-per-revolution displacement samples recorded. The results are shown in Figure 12. A dramatic increase in variance is seen once the stability limit of approximately 72 μm is exceeded. This suggests that abrupt discontinuities in variance could be used to locate stability boundaries. As an example, we have calculated the variance in the (simulated) synchronously sampled tool point displacement over a grid of spindle speeds (11000 rpm to 17000 rpm) and axial depths (0.01 mm to 0.3 mm) for the 9:1 tooling. The resulting 2-D surface plot is shown in Figure 13. A comparison of this figure with the analytic stability lobe (plotted on the same scale) shown in Figure 14 indicates that the statistical variance in the once-per-revolution displacement signal may be a good indicator of the onset of chatter and could be used to construct time-based stability lobes, similar to the peak-to-peak diagrams described by Smith and Tlusty [7].

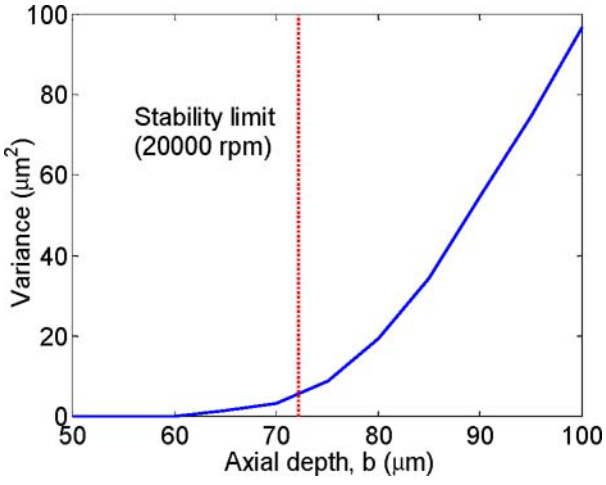

Figure 12: Axial depth vs. variance for 9:1 tooling.

3 SUMMARY

This paper details recent research focused on the rapid identification of the tool point frequency response and/or stable cutting parameters for high-speed machining. Three new techniques were discussed. First, pre-process determination of optimum spindle speeds using the combination of a magnet in close proximity to the tool point to produce a non-contact periodic excitation, tool point displacement measurements, and once-per-revolution sampling was described (referred to as the *best speeds device*). Experimental results showed that synchronous sampling of the tool point displacement at peak force during spindle speed ramping allowed calculation of qualitative representations of the real part of the system frequency response and corresponding stability lobes. This information, in turn, allowed intelligent selection of optimum spindle speed(s). The predicted best speeds were verified by impact testing. Additionally, it was suggested that if the magnet force were also recorded, quantitative descriptions of the real part of the system FRF and resulting stability lobes would be possible.

Second, an example of Receptance Coupling Substructure Analysis (RCSA) for the pre-process analytic prediction of the tool point response was described. It was shown that the RCSA model provides the ability to select the overhang length (within the allowable range for a particular tool) to achieve optimum material removal rate. Machining tests verified the method.

Finally, once-per-revolution sampling of the audio signal during cutting and analysis of the resulting point distribution (e.g., using a histogram and/or the statistical variance) to determine stability behavior was described. Experimental results demonstrated a large increase in

the statistical variance of the once-per-revolution audio data from stable to unstable cutting conditions. Milling simulation code was also developed to calculate the variance in the synchronously sampled tool point displacement over a range of spindle speeds and chip widths. It was shown that this information could be used to construct plots that indicate stable/unstable behavior, similar to the well-known stability lobe and peak-to-peak diagrams.

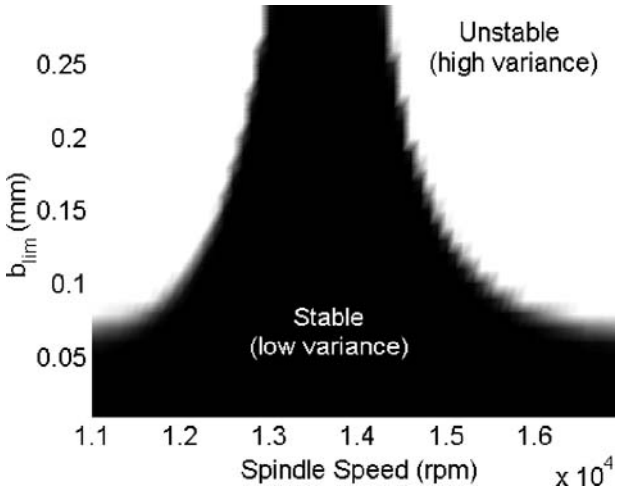

Figure 13: Variance surface plot for 9:1 tooling showing stable (dark) and unstable (light) regions.

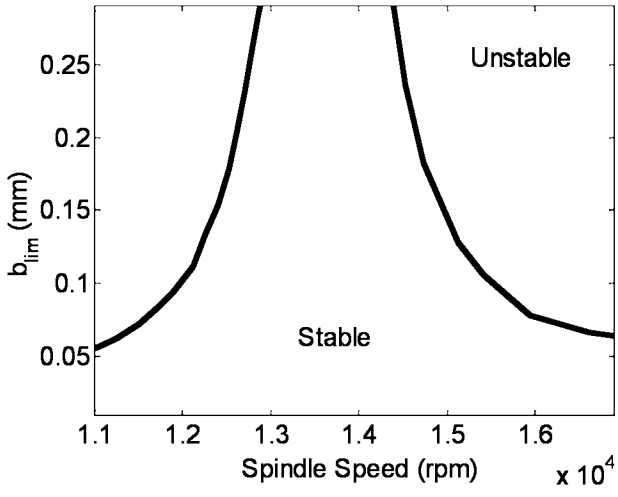

Figure 14: Analytic stability lobes for 9:1 tooling.

4 ACKNOWLEGEMENTS

The authors gratefully acknowledge support from an NRC/NIST Postdoctoral Research Fellowship (for T. Schmitz).

5 REFERENCES

[1] Smith, S., Tlusty, J., 1990, Update on High-Speed Milling Dynamics, Transactions of the ASME Journal of Engineering for Industry, 112: 142-149.

[2] Schultz, H., Moriwaki, T., 1992, High-Speed Machining, Annals of the CIRP, 41/2: 637-643.

[3] Merrit, H., 1965, Theory of Self-Excited Machine Tool Chatter, Transaction of the ASME Journal of Engineering for Industry, 87: 447-454.

[4] Minis, I., Yanushevsky, T., Tembo, R., Hocken, R., 1990, Analysis of Linear and Nonlinear Chatter in Milling, Annals of the CIRP, 39/1: 459-462.

[5] Altintas, Y., Lee, P., 1996, A General Mechanics and Dynamics Model for Helical End Mills, Annals of the CIRP, 45/1: 59-64.

[6] Budak, E., Altintas, Y., 1998, Analytical Prediction of Chatter Stability Conditions for Multi-Degree of Freedom Systems in Milling, Part I: Modeling, Part II: Applications, Transactions of the ASME Journal of Dynamic Systems, Measurement and Control, 120: 22-36.

[7] Smith, S., Tlusty, J., 1991, An Overview of Modeling and Simulation of the Milling Process, Transactions of the ASME Journal of Engineering for Industry, 113: 169-175.

[8] Smith, S., Tlusty, J., 1992, Stabilizing Chatter by Automatic Spindle Speed Regulation, Annals of the CIRP, 41/1: 433-436.

[9] Smith, S., Explosive Excitation Method and Device, Application for U.S. Patent, submitted April 2000.

[10] Davies, M., Dutterer, B., Pratt, J., Device for Stable Speed Determination in Machining, Application for U.S. Patent, NIST Docket #99-016/025US.

[11] Koenisberger, F., Tlusty, J., 1967, Machine Tool Structures-Vol. I: Stability Against Chatter, Pergamon Press, 202-203.

[12] http://www.mfg-labs.com/Harmonizer.

[13] Schmitz, T., Donaldson, R., 2000, Predicting High-Speed Machining Dynamics by Substructure Analysis, Annals of the CIRP, 49/1: 303-308.

[14] Ferreira, J., Ewins, D., 1995, Nonlinear Receptance Coupling Approach Based on Describing Functions, Proceedings of the 14th International Modal Analysis Conference, Dearborn, MI, 1034-1040.

[15] Ren, Y., Beards, C., 1993, A Generalized Receptance Coupling Technique, Proceedings of the 11th International Modal Analysis Conference, Kissimmee, FL, 868-871.

[16] Klosterman, A., McClelland, W., Sherlock, I., 1977, Dynamic Simulation of Complex Systems Utilizing Experimental and Analytical Techniques, ASME, 75-WA/Aero-9.

[17] Tlusty, J., Smith, S., Winfough, W., 1996, Techniques for the Use of Long Slender End Mills in High-Speed Machining, Annals of the CIRP, 45/1: 393-396.

[18] Davies, M., Dutterer, B., Pratt, J., Schaut, A., 1998, On the Dynamics of High-Speed Milling with Long, Slender Endmills, Annals of the CIRP, 47/1: 55-60.

[19] Smith, S., Winfough, W., Halley, J., 1998, The Effect of Tool Length on Stable Metal Removal Rate in High-Speed Milling, Annals of the CIRP, 47/1: 307-310.

[20] Smith, S., Winfough, W., Bochers, H., 2000, Power and Stability Limits in Milling, Annals of the CIRP, 49/1: 309-312.

[21] Blevins, R., 1979, Formulas for Natural Frequency and Mode Shape, Van Nostrand Reinhold Co., New York, NY.

[22] Winfough, W., Smith, S., 1995, Automatic Selection of the Optimum Metal Removal Conditions for High-Speed Milling, Transactions of the NAMRI/SME, 23: 163-168.

[23] Tlusty, J., 2000, Manufacturing Processes and Equipment, Prentice Hall, Upper Saddle River, NJ, 570-579.